Chapter 2
The Density Matrix Renormalization Group

Adrian E. Feiguin

Abstract Since its creation in 1992, the density matrix renormalization group (DMRG) method has evolved and mutated. From its original formulation in a condensed matter context, it has been adapted to study problems in various fields, such as nuclear physics and quantum chemistry, becoming one of the dominant numerical techniques to simulate strongly correlated systems. In this chapter, we shall cover many technical aspects of the DMRG, from a "traditional", or "conventional" perspective, describing the theoretical fundamentation, as well as the details of the algorithm.

2.1 Introduction

Variational methods rely on a trial wave function or ansatz derived from some physical insight. This wave-function may, or may not describe the actual ground state of a system, but if it does—even in an approximate way—we may gain some enormous knowledge. The Bethe ansatz is actually exact when applied to an integrable model, but it can also be an approximation such as in the case of $SU(N)$ models [1–3]. Laughlin's wave-function for the fractional quantum Hall state at filling fraction $\nu = 1/3$ has more than 95 % accuracy [4]. The Hartree-Fock method can be formulated as a variational ansatz, as well as the BCS theory of superconductivity [5].

The Density Matrix Renormalization Group (DMRG) method [6, 7] is variational, but relies heavily on exact diagonalization and numerical renormalization group (NRG) ideas. It was introduced by Steve White in 1992 as a development of Wilson's NRG [8, 9]. The premise is to obtain a wave-function that approximates the actual ground-state in a reduced Hilbert space, minimizing the loss of information. In a

A. E. Feiguin (✉)
Department of Physics, Northeastern University, Boston, MA 02115, USA
e-mail: a.feiguin@neu.edu

A. Avella and F. Mancini (eds.), *Strongly Correlated Systems*,
Springer Series in Solid-State Sciences 176, DOI: 10.1007/978-3-642-35106-8_2,

certain way, it can be considered as an algorithm to compress the wave-function, same as classical compression algorithms work in digital imaging.

It is variational because the proposed solution has the very peculiar form of a "matrix-product state" (MPS) [10–13], and it also involves a truncation of the basis. However, no a priori assumptions are made about the form of the coefficients, or the underlying physics. The power of the method is precisely that it is "smart" enough to be able to find for us the best possible wave-function of that form, without any "external bias". Even though the accuracy is finite, it is totally under control, and we can obtain results that are essentially exact (also referred-to as "quasi-exact"). Another ingredient is a block decimation process, similar to the one introduced by Wilson. However, the NRG technique has very limited applicability, while the DMRG can be used for a wide range of lattice problems.

The DMRG possesses features that make it extremely powerful: it is able to treat very large systems with hundreds of degrees of freedom, and to provide the most accurate results for ground-state energies and gaps in low dimensional systems. Reviews on the DMRG method abound [14–20]. For detailed lecture notes, we refer the reader to Refs. [18, 20].

2.2 Truncated Diagonalization: The Numerical Renormalization Group Idea

In this section we introduce the concept of "truncated diagonalization". The idea is to diagonalize the Hamiltonian in a constrained Hilbert space. The questions to address are: how do we pick the states to keep, and the states to discard? Does this choice depend on the representation? Can we quantify the amount of "information" lost in the process? We shall start by describing a pretty unconventional diagonalization procedure that will help us introduce the main tools needed to build the DMRG algorithm. For illustration purposes we shall consider a one-dimensional chain of quantum spins described by the Heisenberg Hamiltonian.

2.2.1 Two-Spin Problem

The Hilbert space for the two-spin problem consists of four possible configurations of two spins

$$\{|\uparrow\uparrow\rangle, |\uparrow\downarrow\rangle, |\downarrow\uparrow\rangle, |\downarrow\downarrow\rangle\} \tag{2.1}$$

The problem is described by the Hamiltonian:

$$\hat{H} = \hat{S}_1^z \hat{S}_2^z + \frac{1}{2}\left[\hat{S}_1^+ \hat{S}_2^- + \hat{S}_1^- \hat{S}_2^+\right] \tag{2.2}$$

The corresponding matrix will have dimensions 4×4. In order to compute this matrix we shall use some simple matrix algebra to first obtain the single-site operators in the expanded Hilbert space. This is done by the following simple scheme: And operator O_1 acting on the left spin, will have the matrix form:

$$\tilde{O}_1 = O_1 \otimes \mathbb{1}_2 \tag{2.3}$$

Similarly, for an operator O_2 acting on the right spin:

$$\tilde{O}_2 = \mathbb{1}_2 \otimes O_2 \tag{2.4}$$

where we introduced the $n \times n$ identity matrix $\mathbb{1}_n$. The product of two operators acting on different sites can be obtained as:

$$\tilde{O}_{12} = O_1 \otimes O_2 \tag{2.5}$$

It is easy to see that the Hamiltonian matrix will be given by:

$$H_{12} = S^z \otimes S^z + \frac{1}{2}\left[S^+ \otimes S^- + S^- \otimes S^+\right] \tag{2.6}$$

where we used the single spin (2×2) matrices S^z and $S^{\pm}$. We leave as an exercise for the reader to show that the final form of the matrix is:

$$H_{12} = \begin{pmatrix} 1/4 & 0 & 0 & 0 \\ 0 & -1/4 & 1/2 & 0 \\ 0 & 1/2 & -1/4 & 0 \\ 0 & 0 & 0 & 1/4 \end{pmatrix}, \tag{2.7}$$

Obtaining the eigenvalues and eigenvectors is also a straightforward exercise: two of them are already given, and the entire problem now reduces to diagonalizing a two by two matrix. We therefore obtain the well known result: The ground state $|s\rangle = 1/\sqrt{2}\,[|\uparrow\downarrow\rangle - |\downarrow\uparrow\rangle]$, has energy $E_s = -3/4$, and the other three eigenstates $\left\{|\uparrow\uparrow\rangle, |\downarrow\downarrow\rangle, 1/\sqrt{2}\left[|\uparrow\downarrow\rangle + |\downarrow\uparrow\rangle\right]\right\}$ form a multiplet with energy $E_t = 1/4$.

2.2.2 Many Spins

Imagine now that we add a third spin to the right of our two spins. We can use the previous result to obtain the new 8×8 Hamiltonian matrix as:

$$H_3 = H_2 \otimes \mathbb{1}_2 + \tilde{S}_2^z \otimes S^z + \frac{1}{2}\left[\tilde{S}_2^+ \otimes S^- + \tilde{S}_2^- \otimes S^+\right] \tag{2.8}$$

Here we used the single spin S_1^z, $S_1^{\pm}$, and the 'tilde' matrices defined in Eqs. (2.3) and (2.4):

$$\tilde{S}_2^z = \mathbb{1}_2 \otimes S^z, \tag{2.9}$$

and

$$\tilde{S}_2^{\pm} = \mathbb{1}_2 \otimes S^{\pm}, \tag{2.10}$$

It is easy to see that this leads to a recursion scheme to construct the $2^i \times 2^i$ Hamiltonian matrix the ith step as:

$$H_i = H_{i-1} \otimes \mathbb{1}_2 + \tilde{S}_{i-1}^z \otimes S^z + \frac{1}{2}\left[\tilde{S}_{i-1}^+ \otimes S^- + \tilde{S}_{i-1}^- \otimes S^+\right] \tag{2.11}$$

with

$$\tilde{S}_{i-1}^z = \mathbb{1}_{2^{i-2}} \otimes S^z, \tag{2.12}$$

and

$$\tilde{S}_{i-1}^{\pm} = \mathbb{1}_{2^{i-2}} \otimes S^{\pm}, \tag{2.13}$$

This recursion algorithm can be visualized as a left 'block', to which we add new 'sites' or spins to the right, one at a time, as shown in Fig. 2.1. The block has a 'block Hamiltonian', H_L, that is iteratively built by connecting to the new spins through the corresponding interaction terms.

The process outlined above leads to a simple and elegant recursion scheme that allows one to construct the Hamiltonian matrix by using simple algebra. However, this idea is very impractical. The basis size, or the linear dimension of the matrix, grows with the number of spins N as 2^N. It is clear that this matrix sizes soon become unmanageable by our computer. One way to deal with this problem is by using the symmetries of the Hamiltonian and the lattice to reduce the Hamiltonian into a block form. This leads to powerful algorithms that can diagonalize dozens of spins. However, this strategy also runs out of steam very soon. Another solution to deal with this exponential growth of the basis can be traced back to Wilson's numerical renormalization group.

Suppose that we are able to diagonalize out Heisenberg spin chain, to obtain the ground state as:

$$|\Psi\rangle = \sum_{s_1,s_2,\ldots,s_N} a_{s_1,s_2,\ldots,s_N} |s_1, s_2, \ldots, s_N\rangle \tag{2.14}$$

where the sum runs over all configurations of N spins. If we plot the weights $|a_{s_1,\ldots,s_N}|^2$ in decreasing order, we may find a structure like the one depicted in the left panel of Fig. 2.2: Most of the weight is concentrated on a couple of configurations, in our case $|\uparrow\downarrow\uparrow\downarrow\ldots\rangle$ and $|\downarrow\uparrow\downarrow\uparrow\ldots\rangle$, and the rest of the weight is spread over a long tail. Usually only a few important states possess most of the weight, especially in ground states that resemble a classical state such as the antiferromagnet. One then might feel inclined to take a pair of scissors, and truncate the basis to a

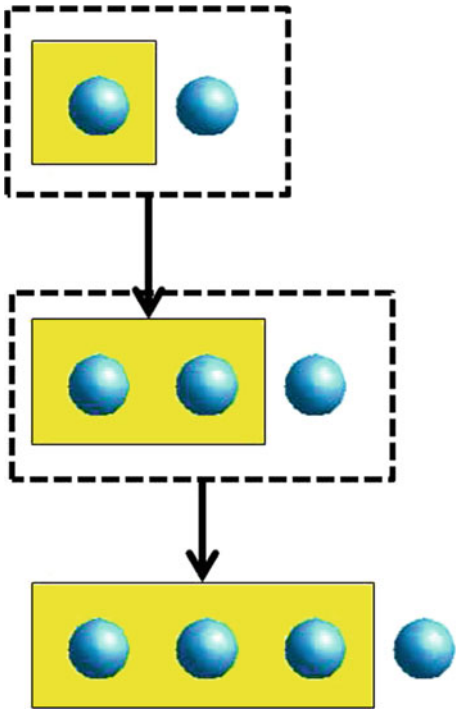

Fig. 2.1 Pictorial representation of the Hamiltonian building recursion explained in the text. At each step, the block size is increased by adding a spin at a time

few dozen states with largest weights, and get rid of the rest. However, this long tail of states with small weights are responsible for most of the interesting physics: the quantum fluctuations, and the difference in weight from one state to another in this tail cannot be necessarily ignored, since they are all of the same order of magnitude.

However, one may notice a simple fact: this is a basis dependent problem! What if, by some smart choice of basis, we find a representation in which the distribution of weights is such that all the weight on the tail is 'shifted to the left' on the plot, as shown on the right panel of Fig. 2.2. Then, if we truncate the basis, we would not need to worry about the loss of 'information'. Of course, this is a nice and simple concept that might work in practice, if we knew how to pick the optimal representation. And as it turns out, this is not in principle an easy task. As we shall learn, what we need is a method for quantifying 'information'.

2.2.3 A Simple Geometrical Analogy

Let us consider a vector in two dimensional space $\boldsymbol{v} = (x, y)$, as shown in Fig. 2.3. We need two basis vectors $\hat{e}_1$ and $\hat{e}_2$ to expand it as $\boldsymbol{v} = x\hat{e}_1 + y\hat{e}_2$. A simple 2D rotation by an angle ϕ would be represented by an orthogonal matrix

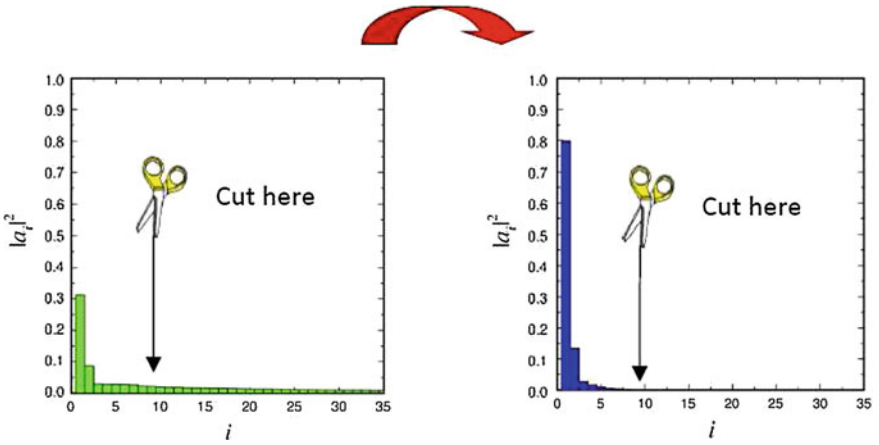

Fig. 2.2 Schematic picture of the ideal basis truncation. Through a change of basis the ground-state weights are more concentrated in a few basis states, such that the loose of information after the truncation is minimal

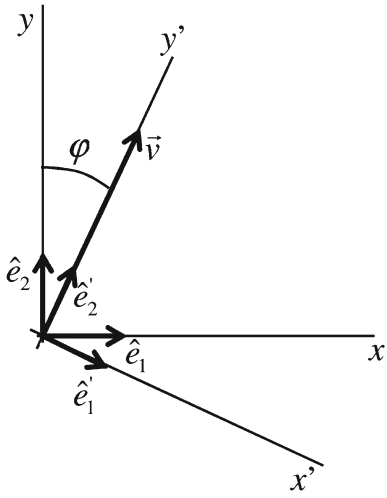

Fig. 2.3 Rotation by an angle ϕ to a new reference system in the 2D plane

$$U = \begin{pmatrix} \cos\phi & \sin\phi \\ -\sin\phi & \cos\phi \end{pmatrix}, \tag{2.15}$$

After such a rotation, the new basis vectors will be $\hat{e}'_1 = \cos\phi\hat{e}_1 + \sin\phi\hat{e}_2$, and $\hat{e}'_2 = -\sin\phi\hat{e}_1 + \cos\phi\hat{e}_2$. If we pick the angle ϕ such that $\boldsymbol{v}$ is aligned along the new y-axis, parallel to $\hat{e}'_2$, we find that we need only one component to describe the vector in the new basis: $\boldsymbol{v} = (0, |v|)$, or $\boldsymbol{v} = |v|\hat{e}'_2$. Therefore, we would feel inclined to eliminating the vector $\hat{e}'_1$ from the basis. After truncating the basis, in order to rotate to the new one-dimensional space, we would use a rotation matrix:

$$U' = \begin{pmatrix} \cos\phi \\ -\sin\phi \end{pmatrix}, \tag{2.16}$$

which still is orthogonal. Now, we clearly see that unless a vector is parallel to $\boldsymbol{v}$, we would loose all information regarding the component orthogonal to $\hat{e}_2'$. In other words, this transformation does not preserve the norm, and therefore, it no longer is unitary. For the case of operators represented by 2×2 matrices in the original basis, we find that they will be reduced to a 1×1 matrix, a scalar, or just a simple change of scale. If we apply an operation on the vector, we have to deal with the fact that there will be some loss of information as a result. We would like to think that this loss of information is minimal, meaning that the contributions with support in the orthogonal manifold are very small. This simplified analogy illustrates the consequences one has to deal with when the basis is truncated.

2.2.4 The Case of Spins

Let us revisit the case of two spins, and look again at the eigenvectors of the Hamiltonian (2.7). By direct inspection we find that the states $|+\rangle = |\uparrow\uparrow\rangle$ and $|-\rangle = |\downarrow\downarrow\rangle$ are already eigenstates with eigenvalues $E_\pm = 1/4$. The other eigenstates can be found by diagonalizing the remaining 2×2 matrix, yielding

$$|s\rangle = \frac{1}{\sqrt{2}}\left[|\uparrow\downarrow\rangle - |\downarrow\uparrow\rangle\right]$$
$$|t\rangle = \frac{1}{\sqrt{2}}\left[|\uparrow\downarrow\rangle + |\downarrow\uparrow\rangle\right]$$

with eigenvalues $E_s = -3/4$ and $E_t = 1/4$ respectively. The transformation matrix, to rotate to this new basis is simple given by the eigenvectors in columns as:

$$U = \begin{pmatrix} 1 & 0 & 0 & 0 \\ 0 & 1/\sqrt{2} & 1/\sqrt{2} & 0 \\ 0 & -1/\sqrt{2} & 1/\sqrt{2} & 0 \\ 0 & 0 & 0 & 1 \end{pmatrix}, \tag{2.17}$$

If we focus on the $|s\rangle$ and $|t\rangle$ states, we see that the 2×2 rotation matrix is equivalent to the geometric rotation Eq. (2.15) with an angle $\phi = -\pi/4$:

$$\hat{e}_1' = \frac{1}{\sqrt{2}}\hat{e}_1 - \frac{1}{\sqrt{2}}\hat{e}_2$$
$$\hat{e}_2' = \frac{1}{\sqrt{2}}\hat{e}_1 + \frac{1}{\sqrt{2}}\hat{e}_2$$

The full transformation occurs in a four-dimensional space, but the two vectors $|+\rangle$ and $|-\rangle$ are untouched. Same as in the geometric case, the transformation preserves the norm (it is unitary!), and angles between basis states (it is an orthogonal transformation!), and we can use the eigenvectors as a new basis in which the Hamiltonian is already diagonal. In the course of these lecture we shall use slightly more complicated rotations, in which the states are eigenstates of a different matrix, not necessarily the Hamiltonian.

Now, we found that we do not need the basis states $|+\rangle$ and $-\rangle$ to obtain the ground-state. By discarding these two states we simplify the calculation by reducing a 4×4 eigenvalue problem to a 2×2 problem. If we knew in advance that the ground-state was in the subspace with $S^z_{total} = 0$ we could have formulated the problem directly in this subspace. This is a "trivial" truncation: if we are interested in a state with particular values of the quantum numbers, and if the Hamiltonian does not mix subspaces with different quantum numbers/symmetries, we can "block diagonalize" the Hamiltonian in each subspace separately.

Notice that the geometric analogy consists, in terms of spins, in truncating the Hilbert space to just one basis state $|s\rangle$ in this case, the eigenvector of the Hamiltonian with the lowest eigenvalue.

2.2.5 The Block Decimation Idea

Let us try a simple idea, using the recursion scheme described above. At every step in the recursion, we add one spin on the right, and our basis dimension grows by a factor 2. At some point during this recursion, the matrix will be too large to deal with. So let us fix a maximum number of states that we want to keep, m. At certain point during the process, the basis dimension will become larger than m. It is here that we start applying the truncation rule: diagonalize the Hamiltonian matrix exactly, and keep only the m states with *lowest* eigenvalues (see Fig. 2.4).

As the system grows, the basis of the left block changes as we rotate to the new basis of eigenstates of the Hamiltonian. This is done by using a unitary transformation U. This matrix U is nothing else but the matrix with the eigenstates ordered in columns. Therefore, adding a spin to the block now involves two steps: (i) we need to build the 'tilde' operators as before, and (ii) rotate the Hamiltonian matrix and the tilde operators to the new basis (Fig. 2.5).

Let us assume that our old block before adding a site has a basis $\{|\alpha_{i-1}\rangle\}$, of dimension D_{i-1}, and the site has a basis $\{|s_i\rangle\}$ of dimension d. The new block basis $\{|\alpha_{i-1}, s_i\rangle\}$ has dimension $d \times D_{i-1}$, such that we can easily diagonalize it to obtain all the eigenvalues and corresponding eigenvectors $\{|\alpha_{i+1}\rangle\}$. We build the matrix U as the $D_{i-1} \times D_i$ unitary matrix with the $D_i = m$ eigenvectors with largest eigenvalues in the columns:

$$U_{\alpha_{i-1}s_i,\alpha_i} = \langle \alpha_{i-1} s_i | \alpha_i \rangle. \tag{2.18}$$

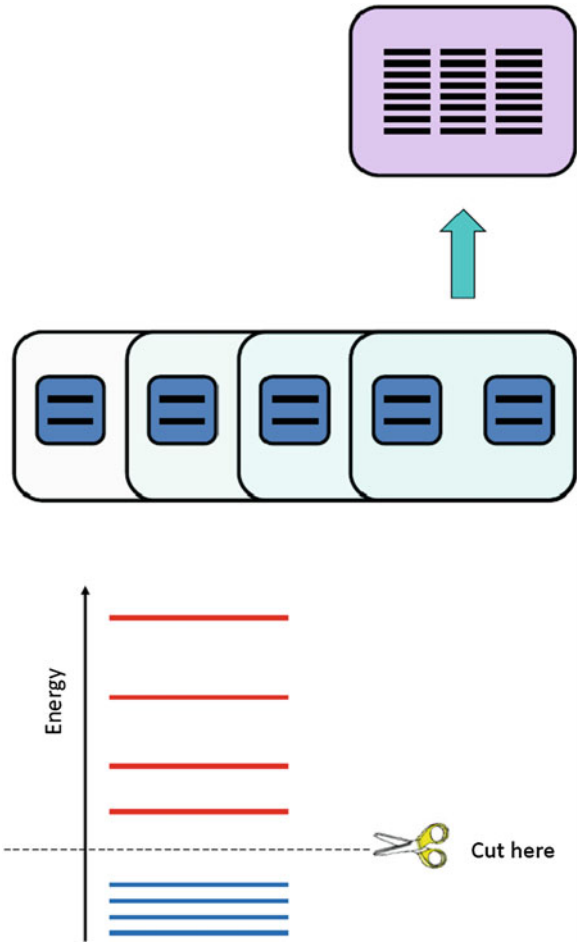

Fig. 2.4 In the NRG scheme, we truncate the basis by keeping the m eigenstates of the Hamiltonian with the lowest eigenvalues

Before the rotation, the operators had matrix elements:

$$\tilde{O}_{\alpha_{i-1}s_i,\alpha'_{i-1}s'_i} = \langle \alpha_{i-1}s_i|\hat{O}|\alpha'_{i-1}s'_i\rangle. \tag{2.19}$$

We can now rotate all the tilde operators to the new basis as:

$$\begin{aligned}\tilde{O}_{\alpha_i,\alpha'_i} &= \langle \alpha_i|\hat{O}|\alpha'_i\rangle = \sum_{\alpha_{i-1},s_i}\sum_{\alpha'_{i-1}s'_i}\langle \alpha_i|\alpha_{i-1}s\rangle\langle \alpha_{i-1}s_i|\hat{O}|\alpha'_{i-1}s'_i\rangle\langle \alpha'_{i-1}s'|\alpha_i\rangle \\ &= \sum_{\alpha_{i-1},s_i}\sum_{\alpha'_{i-1}s'_i}(U^\dagger)_{\alpha_i,\alpha_{i-1}s_i}\tilde{O}_{\alpha_i\alpha'_i}U_{\alpha'_{i-1}s'_i,\alpha'_i}\end{aligned} \tag{2.20}$$

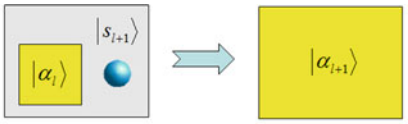

$$|\alpha_{l+1}\rangle = \sum_{s_{l+1},\alpha_l} \langle \alpha_l s_{l+1} | \alpha_{l+1} \rangle |\alpha_l\rangle \otimes |s_{l+1}\rangle = \sum_{s_{l+1},\alpha_l} \left(U_L^{l+1}\right)_{\alpha_l s_{l+1},\alpha_{l+1}} |\alpha_l\rangle \otimes |s_{l+1}\rangle$$

Fig. 2.5 Adding a site to a block now involves a truncation and a change of basis

where the new matrices will have dimensions $m \times m$. we can now use these matrices to continue to block-growing process by adding another site. This can be repeated until the energy per site converges, or until we reach a desired system size.

It may seem that this new basis would be a natural choice is we assume that the physics of the problem is described by different manifolds with different energy scales. If we keep the lowest energy states and we get rid of the high energy states we can expect to get the low energy physics right. This in fact is the case in problems such as the Kondo and Anderson impurity problems [21]. However, in strongly correlated, many-body problems such as the Heisenberg chain, this scheme performs poorly.

2.3 The Density Matrix Truncation: The Kernel of the DMRG

The problem was solved by Steve White by using what he called the 'density matrix truncation'. He realized (without knowing at the time) that instead of getting rid of high energy states, one has to redistribute the 'entanglement' and minimize the loss of information. However, the way he formulated the problem did not incorporate the idea of entanglement, a concept that entered the picture much later after quantum information ideas were used to understand why and when the DMRG actually works. Before introducing these ideas, we shall describe the original formulation of the density matrix truncation [6, 7].

In order to introduce this new concept, we are going to use a new scheme: We are going to use two blocks instead of one, a left block, and a right block, as shown in Fig. 2.6. We are going to grow both blocks simultaneously using the same procedure outlined previously: at every step we add one site at the right of the left block, and one site to the left of the right block. The ground state can then be written as:

$$|\Psi\rangle = \sum_{i,j} \Psi_{ij} |i\rangle |j\rangle, \tag{2.21}$$

where the sum runs over all the states of the left block $|i\rangle$ and right block $|j\rangle$, with the corresponding coefficients Ψ_{ij}.

Now the idea is as follows: once we reach the desired basis dimension m, we shall rotate the left block to a new basis $|i\rangle \rightarrow |\alpha\rangle$. We want to pick these states $|\alpha\rangle$ in such

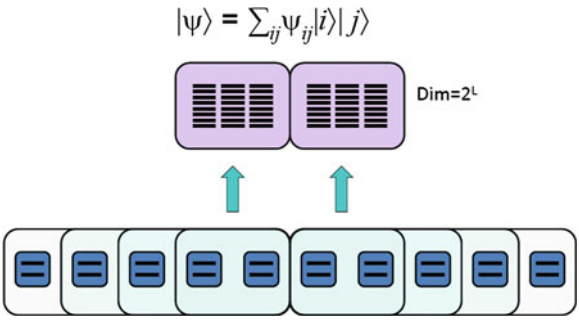

Fig. 2.6 The DMRG modifies the NRG idea by adding a second block

a way that when we truncate the basis, the "distance" between the original ground state $|\Psi\rangle$, and the new, truncated, variational approximation $|\tilde{\Psi}\rangle$, is minimized:

$$S = \left| |\Psi\rangle - |\tilde{\Psi}\rangle \right|^2, \tag{2.22}$$

where

$$|\tilde{\Psi}\rangle = \sum_{\alpha=1}^{m} \sum_{j} \Psi_{\alpha j} |\alpha\rangle |j\rangle. \tag{2.23}$$

We are going to anticipate the solution: pick the basis $|\alpha\rangle$ given by the m eigenvectors of the reduced density matrix of the left block with the m largest eigenvalues. In order to justify this result, we first need to introduce some important concepts.

2.3.1 The Reduced Density Matrix

Imagine that we have a bipartite system, composed by subsystem A and subsystem B, as shown in Fig. 2.7. The Hilbert space of the system $A + B$ will be given by the tensor product of the Hilbert spaces of the two subsystems: $H_{A+B} = H_A \otimes H_B$, and will have dimension $D_{A+B} = D_A \times D_B$. Assume that the state of our system is described by a normalized wave-function $|\Psi\rangle$ that has support on H_{A+B}. We define

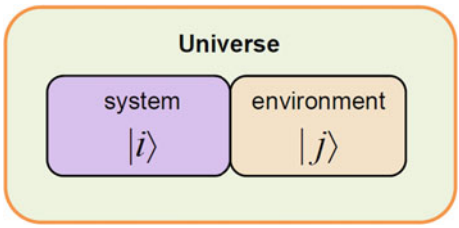

Fig. 2.7 In the DMRG, one block acts as the environment for the second one

the reduced density matrix of subsystem A as

$$\hat{\rho}_A = \mathrm{Tr}_B |\Psi\rangle\langle\Psi|. \tag{2.24}$$

Its corresponding matrix form is

$$\rho_{A\,ii'} = \langle i|\hat{\rho}_A|i'\rangle = \sum_j \langle ij|\Psi\rangle\langle\Psi|i'j\rangle = \sum_j \Psi_{ij}\Psi^*_{i'j} \tag{2.25}$$

This operator describes the density matrix of a mixed state, in which the system A is in contact with a bath or environment B. This is the price we have to pay for our ignorance of subsystem B.

The reduced density matrix has some nice properties:

- It is Hermitian (or symmetric in case of real matrices). This means that its eigenvalues are real.
- Its eigenvalues are non-negative.
- The trace equals to unity: $\mathrm{Tr}\rho_\mathrm{A} = 1$.
- Its eigenvectors $|\alpha\rangle$ and eigenvalues ω_α form an orthonormal basis.

This means that the reduced density matrix can be re-defined in the new eigenvector basis as:

$$\hat{\rho}_A = \sum_\alpha \omega_\alpha |\alpha\rangle\langle\alpha|; \tag{2.26}$$

with $\omega_\alpha \geq 0$ and $\sum_\alpha \omega_\alpha = 1$.

These same considerations are valid for the block B.

Exercise: Given a state $|\Psi\rangle$ defined in $A + B$, show that the mean value of an observable $\hat{O}_A$ acting on subsystem A, can be obtained as $\langle\Psi|\hat{O}_A|\Psi\rangle = \mathrm{Tr}\rho_A O_A$.

2.3.2 The Singular Value Decomposition

Consider an arbitrary matrix Ψ of dimensions $D_A \times D_B$. One can prove that Ψ can be factorized as

$$\Psi = UDV^\dagger, \tag{2.27}$$

where U is a $(D_A \times D_B)$ unitary matrix, V is a $(D_B \times D_B)$ unitary matrix, and D is a $(D_B \times D_B$ diagonal matrix with real non-negative numbers along the diagonal, and zeroes elsewhere. Since U and V are unitary, they satisfy:

$$UU^\dagger = \mathbb{1};$$

$$VV^\dagger = \mathbb{1}.$$

Their columns are orthonormal vectors, so U and V can be regarded as rotation matrices. The diagonal matrix elements λ_α of D are known as the "singular values" of Ψ.

2.3.3 The Schmidt Decomposition

Let us apply the SVD to our quantum wave-function $|\Psi\rangle$ (2.21), and for illustration, let us assume that $D_B \leq D_A$. The coefficients Ψ_{ij} define a matrix Ψ. After a SVD, they can be re-written as:

$$\Psi_{ij} = \sum_\alpha^{D_B} U_{i\alpha}\lambda_\alpha (V^\dagger)_{\alpha j} = \sum_\alpha^{D_B} U_{i\alpha}\lambda_\alpha V^*_{\alpha j}. \tag{2.28}$$

The wave-function can now be expressed as:

$$\begin{aligned}
|\Psi\rangle &= \sum_i^{D_A}\sum_j^{D_B}\sum_\alpha^{D_B} U_{i\alpha}\lambda_\alpha V^*_{\alpha j}|i\rangle|j\rangle \\
&= \sum_\alpha^{D_B}\left(\sum_i^{D_A} U_{i\alpha}|i\rangle\right)\lambda_\alpha\left(\sum_j^{D_B} V^*_{\alpha j}|j\rangle\right) \\
&= \sum_\alpha^{D_B}\lambda_\alpha|\alpha\rangle_A|\alpha\rangle_B,
\end{aligned}$$

where we have defined the states $|\alpha\rangle_A = \sum_i U_{i\alpha}|i\rangle$ and $|\alpha\rangle_B = \sum_j V^*_{\alpha j}|j\rangle$. Due to the properties of U and V, these states define a new orthogonal basis. This final expression is known as the "Schmidt decomposition" of the state Ψ, and the bases $|\alpha\rangle$ as the "Schmidt bases".

In general, we have that the state Ψ can be written in the new basis as:

$$|\Psi\rangle = \sum_\alpha^r \lambda_\alpha|\alpha\rangle_A|\alpha\rangle_B; \quad r = \min(D_A, D_B). \tag{2.29}$$

In the Schmidt basis, the reduced density matrices for the subsystems A and B are

$$\rho_A = \mathrm{Tr}|\Psi\rangle\langle\Psi| = \sum_\alpha \lambda_\alpha^2|\alpha\rangle_A\,{}_A\langle\alpha|, \tag{2.30}$$

and

$$\rho_B = \sum_\alpha \lambda_\alpha^2 |\alpha\rangle_B \, {}_B\langle\alpha| \tag{2.31}$$

At this point, we realize some interesting observations:

- The eigenvalues of the reduced density matrices are $\omega_\alpha = \lambda_\alpha^2$, the square of the singular values.
- The two reduced density matrices share the spectrum.
- The Schmidt bases are the eigenvectors of the reduced density matrices.

2.3.4 Optimizing the Truncated Wave-Function

We here go back to the original problem of optimizing the wave-function in a reduced basis. In order to solve it, we are going to reformulate the question as: Given a matrix Ψ, what is the optimal matrix $\tilde{\Psi}$ with fixed rank m that minimizes the Frobenius distance between the two matrices? It turns out, this is a well known problem called the "low ranking approximation".

If we order the eigenvalues of the reduced density matrix in decreasing order $\omega_1, \omega_2, \ldots \omega_m, \ldots \omega_r$, it is straightforward to see that the Frobenius distance between the two matrices is given by

$$S = \left|\Psi - \tilde{\Psi}\right|^2 = \sum_{m+1}^{r} \omega_i \tag{2.32}$$

This proves that the optimal basis is given by the eigenvectors of the reduced density matrix with the m largest eigenvalues.

2.4 Infinite-Size DMRG

The above considerations allow us now to introduce the DMRG algorithm in a very natural way. We are going to present it in the traditional formulation, starting with the infinite-size algorithm, followed by the finite-size scheme.

The main idea behind the infinite-size algorithm consists in growing the left and right blocks by adding one site at a time. As we add sites, the basis of the blocks will grow, until we reach the desired maximum number of states m. At this point we need to start applying the density matrix truncation on both blocks. This process is repeated until we reach a desired system-size, or the error in the energy is below a pre-defined tolerance.

The algorithm illustrated in Fig. 2.8 could be outlined as below:

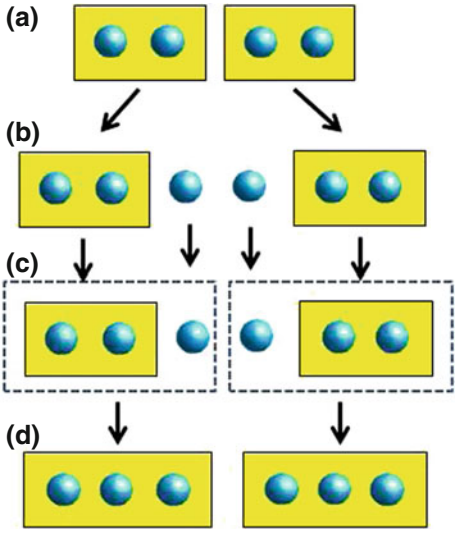

Fig. 2.8 Step-by-step illustration of the block-growing scheme in the infinite-size DMRG algorithm: After obtaining the new blocks from the previous step (**a**), we add a new site to each block (**b**), we build the superblock and obtain the ground-state (**c**), and we calculate the reduced density-matrix, and rotate to the basis of the eigenvectors with m largest eigenvalues to build the new blocks for the next step (**d**)

- Build all the operator matrices for a single-site Hamiltonian, and the operators involved in the interactions between the site an the rest of the system.
- Start growing the blocks by adding single-sites, as outlined in the exact diagonalization section. We assume that the Hilbert space for the single site has dimension d.
- When the size of the bocks become larger than $d \times m$, we start applying the density matrix truncation as follows:

  1. Using a suitable library routine (Lanczos, Davidson), diagonalize the full Hamiltonian (sometimes called super-Hamiltonian) of the two blocks combined (sometimes refereed to as superblock), to obtain the ground state $|\Psi\rangle = \sum_{ij} \Psi_{ij} |i\rangle |j\rangle$.
  2. Calculate the reduced density matrix of the left block, and right blocks. When the system is symmetric under reflections, we only need one of them.
  3. For each of the blocks, diagonalize the density matrix to obtain the full spectrum and eigenvectors.
  4. Truncate the basis by keeping only the m eigenvectors with the largest eigenvalues.
  5. Rotate the Hamiltonian and the operators involved in the interactions between blocks to the new basis.
  6. Add a new site to the left and right blocks, to build new blocks of dimension $d \times m$, and reiterate the diagonalization and truncation steps. Stop when we reach the desired system-size, or the error in the energy is below a pre-defined tolerance.

In the early days of DMRG it was assumed that this scheme would lead to a good approximation of the system properties in the thermodynamic limit. Today we know that he best way to reach the thermodynamic limit is by using the finite-size algorithm on systems of fixed length, and doing a careful finite-size analysis of the results.

Let us now explain some of these steps in more detail.

2.4.1 Adding a Single Site to the Block

Same as we did in the exact diagonalization section, we can add sites to the blocks by performing tensor products of the "tilde" operators on the block, and single-site operators.

Assume that we are in the ith iteration of the algorithm, with our left and right blocks having length i. Let us label our D_L basis states for the left block $\{|\alpha_i\rangle\}$, and our d basis states for the single site that comes to the right $\{|s_{i+1}\rangle\}$ (see Fig. 2.9). When we add the site to the block, we obtain a new basis for the new combined block as $|\alpha_{i+1}\rangle = |\alpha_i\rangle \otimes |s_{i+1}\rangle$.

Let us assume for illustration purposes that we are dealing once more with the Heisenberg chain. All these ideas can be easily generalized to arbitrary models. Same as we did in the exact diagonalization section, we obtain the new Hamiltonian matrix for the combined block as:

$$H_{L,i+1} = H_{L,i} \otimes \mathbb{1}_2 + \tilde{S}^z_{L,i} \otimes S^z + \frac{1}{2}\left(\tilde{S}^+_{L,i} \otimes S^- + \tilde{S}^-_{L,i} \otimes S^+\right). \tag{2.33}$$

In this expression, the "tilde" operators are in the $|\alpha_i\rangle$ basis, while the others are defined in the single-site basis.

A similar expression applies to the right block, which is obtained from the single site at position $i+2$, with basis $\{|s_{i+2}\rangle\}$ and dimension d, and the right block with

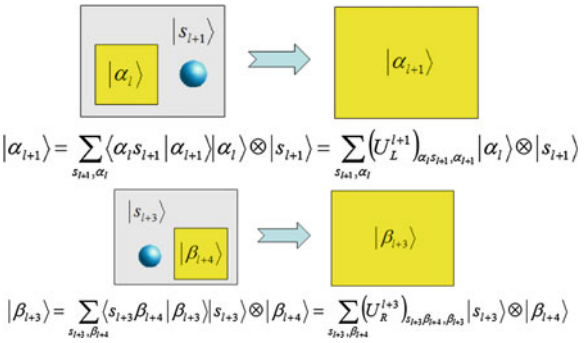

Fig. 2.9 Adding sites to the blocks is done in the same way as in the NRG

basis $\{|\beta_{i+3}\rangle\}$ and dimension D_R:

$$H_{R,i+2} = \mathbb{1}_2 \otimes H_{R,i+3} + S^z \otimes \tilde{S}^z_{R,i+3} + \frac{1}{2}\left(S^+ \otimes \tilde{S}^-_{R,i+3} + S^- \otimes \tilde{S}^+_{R,i+3}\right). \quad (2.34)$$

2.4.2 Building the Super-Hamiltonian

We now need to combine the left and right blocks to form the super-Hamiltonian:

$$\hat{H} = \hat{H}_{L,i+1} + \hat{H}_{R,i+2} + S^z_{i+1} S^z_{i+2} + \frac{1}{2}\left(S^+_{i+1} S^-_{i+2} + S^-_{i+1} S^+_{i+2}\right) \quad (2.35)$$

where $\hat{H}_{L(R)}$ where obtained above, and only involve terms in the left (right) block. The single sites at positions $i+1$ and $i+2$ were absorbed by the left and right blocks, respectively, so in order to build the interactions, we have to rotate the corresponding operators to the new basis of the blocks. This is again done in the same spirit of the "tilde" transformation:

$$\begin{aligned} H = {} & H_{L,i+1} \otimes \mathbb{1}_{D_R \times 2} + \mathbb{1}_{D_L \times 2} \otimes H_{R,i+2} \\ & + \mathbb{1}_{D_L} \otimes S^z \otimes S^z \otimes \mathbb{1}_{D_R} \\ & + \frac{1}{2}\mathbb{1}_{D_L} \otimes S^+ \otimes S^- \otimes \mathbb{1}_{D_R} \\ & + \frac{1}{2}\mathbb{1}_{D_L} \otimes S^- \otimes S^+ \otimes \mathbb{1}_{D_R} \end{aligned}$$

or:

$$\begin{aligned} H = {} & H_{L,i+1} \otimes \mathbb{1}_{D_R \times 2} + \mathbb{1}_{D_L \times 2} \otimes H_{R,i+2} \\ & + \tilde{S}^z_{L,i+1} \otimes \tilde{S}^z_{R,i+2} \\ & + \frac{1}{2}\tilde{S}^+_{L,i+1} \otimes \tilde{S}^-_{R,i+2} \\ & + \frac{1}{2}\tilde{S}^-_{L,i+1} \otimes \tilde{S}^+_{R,i+2} \end{aligned}$$

2.4.3 Obtaining the Ground-State: Lanczos Diagonalization

Once we have a superblock matrix, we can apply a library routine to obtain the ground state of the superblock $|\Psi\rangle$. The two algorithms widely used for this purpose are the Lanczos and Davidson diagonalization. Both are explained to great extent in Ref. [18], so we refer the reader to this material for further information. In these notes we will briefly explain the Lanczos procedure.

The basic idea of the Lanczos method [22, 23] is that a special basis can be constructed where the Hamiltonian has a tridiagonal representation. This is carried out iteratively as shown below. First, it is necessary to select an arbitrary seed vector $|\phi_0\rangle$ in the Hilbert space of the model being studied. If we are seeking the ground-state of the model, then it is necessary that the overlap between the actual ground-state $|\psi_0\rangle$, and the initial state $|\phi_0\rangle$ be nonzero. If no "a priori" information about the ground state is known, this requirement is usually easily satisfied by selecting an initial state with *randomly* chosen coefficients in the working basis that is being used. If some other information of the ground state is known, like its total momentum and spin, then it is convenient to initiate the iterations with a state already belonging to the subspace having those quantum numbers (and still with random coefficients within this subspace).

After $|\phi_0\rangle$ is selected, define a new vector by applying the Hamiltonian $\hat{H}$, over the initial state. Subtracting the projection over $|\phi_0\rangle$, we obtain

$$|\phi_1\rangle = \hat{H}|\phi_0\rangle - \frac{\langle\phi_0|\hat{H}|\phi_0\rangle}{\langle\phi_0|\phi_0\rangle}|\phi_0\rangle, \tag{2.36}$$

that satisfies $\langle\phi_0|\phi_1\rangle = 0$. Now, we can construct a new state that is orthogonal to the previous two as,

$$|\phi_2\rangle = \hat{H}|\phi_1\rangle - \frac{\langle\phi_1|\hat{H}|\phi_1\rangle}{\langle\phi_1|\phi_1\rangle}|\phi_1\rangle - \frac{\langle\phi_1|\phi_1\rangle}{\langle\phi_0|\phi_0\rangle}|\phi_0\rangle. \tag{2.37}$$

It can be easily checked that $\langle\phi_0|\phi_2\rangle = \langle\phi_1|\phi_2\rangle = 0$. The procedure can be generalized by defining an orthogonal basis recursively as,

$$|\phi_{n+1}\rangle = \hat{H}|\phi_n\rangle - a_n|\phi_n\rangle - b_n^2|\phi_{n-1}\rangle, \tag{2.38}$$

where $n = 0, 1, 2, \ldots$, and the coefficients are given by

$$a_n = \frac{\langle\phi_n|\hat{H}|\phi_n\rangle}{\langle\phi_n|\phi_n\rangle}, \qquad b_n^2 = \frac{\langle\phi_n|\phi_n\rangle}{\langle\phi_{n-1}|\phi_{n-1}\rangle}, \tag{2.39}$$

supplemented by $b_0 = 0$, $|\phi_{-1}\rangle = 0$. In this basis, it can be shown that the Hamiltonian matrix becomes,

$$H = \begin{pmatrix} a_0 & b_1 & 0 & 0 & \ldots \\ b_1 & a_1 & b_2 & 0 & \ldots \\ 0 & b_2 & a_2 & b_3 & \ldots \\ 0 & 0 & b_3 & a_3 & \ldots \\ \vdots & \vdots & \vdots & \vdots & \end{pmatrix} \tag{2.40}$$

i.e. it is tridiagonal as expected. Once in this form the matrix can be diagonalized easily using standard library subroutines. However, note that to diagonalize com-

pletely a Hamiltonian on a finite cluster, a number of iterations equal to the size of the Hilbert space (or the subspace under consideration) are needed. In practice this would demand a considerable amount of CPU time. However, one of the advantages of this technique is that accurate enough information about the ground state of the problem can be obtained after a small number of iterations (typically of the order of $\sim$100 or less).

Another way to formulate the problem is by obtaining the tridiagonal form of the Hamiltonian starting from a Krylov basis, which is spanned by the vectors

$$\left\{|\phi_0\rangle, \hat{H}|\phi_0\rangle, \hat{H}^2|\phi_0\rangle, \ldots, \hat{H}^n|\phi_0\rangle\right\} \tag{2.41}$$

and asking that each vector be orthogonal to the previous two. Notice that each new iteration of the process requires one application of the Hamiltonian. Most of the time this simple procedure works for practical purposes, but care must be payed to the possibility of losing orthogonality between the basis vectors. This may happen due to the finite machine precision. In that case, a re-orthogonalization procedure may be required.

Notice that the new super-Hamiltonian matrix has dimensions $D_L D_R d^2 \times D_L D_R d^2$. This could be a large matrix. In state-of-the-art simulations with a large number of states, one does not build this matrix in memory explicitly, but applies the operators to the state directly in the diagonalization routine.

2.4.4 Density Matrix Truncation and the Rotation to the New Basis

The truncation process is similar to the one use in numerical renormalization group, but instead of using the matrix of eigenvectors of the Hamiltonian, we use the eigenvectors $\{|\alpha\rangle\}$, $\{|\beta\rangle\}$ of the left and right reduced density matrix. Therefore, the new basis states for the left and right block are related to the states in the previous step as:

$$\begin{aligned}
|\alpha_{i+1}\rangle &= \sum_{s_{i+1},\alpha_i} \langle \alpha_i s_{i+1}|\alpha_{i+1}\rangle |\alpha_i s_{i+1}\rangle = \sum_{s_{i+1},\alpha_i} (U_L)_{\alpha_i s_{i+1},\alpha_{i+1}} |\alpha_i s_{i+1}\rangle \\
|\beta_{i+2}\rangle &= \sum_{s_{i+2},\beta_{i+3}} \langle s_{i+2}\beta_{i+3}|\beta_{i+2}\rangle |s_{i+2}\beta_{i+3}\rangle = \sum_{s_{i+2},\beta_{i+3}} (U_R)_{s_{i+2}\beta_{i+3},\beta_{i+2}} |s_{i+2}\beta_{i+3}\rangle
\end{aligned} \tag{2.42}$$

where

$$(U_L)_{\alpha_i s_{i+1},\alpha_{i+1}} = \langle \alpha_i s_{i+1}|\alpha_{i+1}\rangle \tag{2.43}$$

and

$$(U_R)_{s_{i+2}\beta_{i+3},\beta_{i+2}} = \langle s_{i+2}\beta_{i+3}|\beta_{i+2}\rangle. \tag{2.44}$$

If we keep only m states, the matrices $U_{L(R)}$ will have dimensions $D_{L(R)}d \times m$. If the basis had already been truncated in the previous step, then $D_L(R) = m$.

We can now use these transformations to obtain the matrix elements for all the operators in the new truncated basis. For instance, an operator acting on a site inside the left block will be transformed as:

$$\begin{aligned}(\tilde{O}_{L,i+1})_{\alpha_{i+1},\alpha'_{i+1}} &= \langle \alpha_{i+1}|\hat{O}|\alpha'_{i+1}\rangle \\ &= \sum_{\alpha_i,s_{i+1}} \sum_{\alpha'_i,s'_{i+1}} \langle \alpha_{i+1}|\alpha_i s_{i+1}\rangle\langle \alpha_i s_{i+1}|\hat{O}|\alpha'_i s'_{i+1}\rangle\langle \alpha'_i s'_{i+1}|\alpha'_{i+1}\rangle \\ &= \sum_{\alpha_i s_{i+1}} \sum_{\alpha'_i s'_{i+1}} (U_L^\dagger)_{\alpha_{i+1},\alpha_i s_{i+1}} (\tilde{O_{L,i}})_{\alpha_i s_{i+1},\alpha'_i s'_{i+1}} (U_L)_{\alpha'_i s'_{i+1},\alpha'_{i+1}},\end{aligned} \tag{2.45}$$

and a similar expression can be obtained for operators in the right block.

2.4.5 Storing Matrices and States

In order to optimize memory usage and performance, we can use the symmetries of the model to store all the matrices in block form. We have already noticed in the two-spin example that we can store the Hamiltonian in block diagonal form, with each block corresponding to a well defined symmetry sector, or quantum number. We can do the same with all our operators, with the main difference being that they may not be diagonal. For instance, the $\hat{S}^z$ operator is diagonal, meaning that it does not mix subspaces with different quantum numbers. The $\hat{S}^+$ operator mixes subspaces with the quantum number S^z differing by $+1$. So we can label the blocks by a pair of quantum numbers or, since we know how the operator changes the quantum numbers, we can use a single index. In the code implementation, we can store the blocks as a list of matrices. The main drawback is that we need a lookup table to find a block with given quantum numbers, but this can be done very efficiently. Notice that this idea can be applied to Hamiltonians that conserve the quantum numbers: if the model mixes different subspaces, we may need to store the full matrix.

The same idea applies to the state vectors. We can store them in a list of arrays, or matrices, each corresponding to a subspace with well defined quantum numbers.

2.5 The Finite-Size DMRG

As we mentioned before, the proper way to reach the thermodynamic limit with DMRG is by studying finite systems and performing a finite-size analysis. In order to study finite system, a generalization of the above ideas needs to be applied. The finite-size DMRG (illustrated in Fig. 2.10) can be summarized as follows:

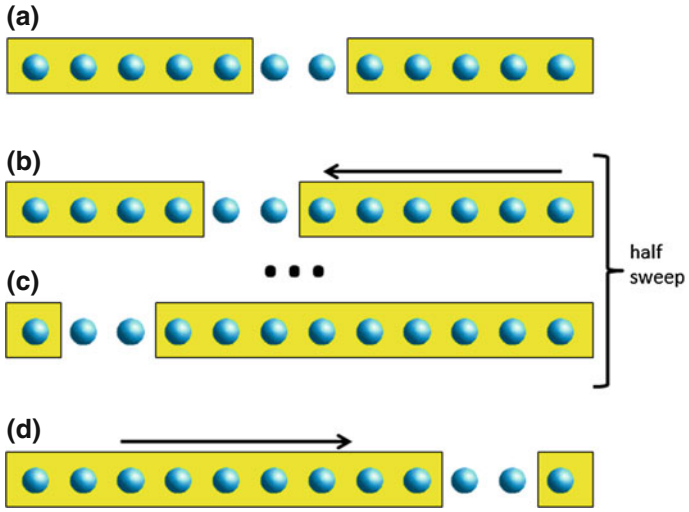

Fig. 2.10 Schematic illustration of the finite-size DMRG algorithm: The infinite-size iteration stops when we reach the desired system size. Then, we start sweeping from left to right, and right to left. During the sweeping iterations, one block grows, and the other one "shrinks". The shrinking block is retrieved from the blocks obtained in the previous sweep in the opposite direction, which are stored in memory or disk

- Run the infinite-size algorithm until the desired system size is reached. During this process, store all the left and right blocks, with their corresponding operators and basis transformations. This step is typically referred to as the "warmup".
- Once the desired system size is reached we start performing "DMRG sweeps", from right-to-left, and left-to-right to optimize the bases and improve accuracy. A left-to-right sweep is described as follows:

  1. Add a site to the left block using the same idea of the infinite-size DMRG. Since the total size of the system needs to be kept fixed, we need to "shrink" the right block. This is done by using the right block from the infinite-size step, or from the previous right-to-left sweep.
  2. Using a suitable library routine (Lanczos, Davidson), diagonalize the super Hamiltonian of the two blocks combined, same as for the infinite-size DMRG.
  3. Calculate the reduced density matrix of the left block.
  4. Diagonalize the density matrix to obtain the full spectrum and eigenvectors.
  5. Truncate the basis by keeping only the m eigenvectors with the largest eigenvalues.
  6. Rotate the Hamiltonian and the operators of the left block involved in the interactions between blocks to the new basis.

7. Iterate until reaching the far right end of the system, with a right block containing a single site. This completes the left-to-right sweep.

- Perform a right-to-left sweep, by growing the right block one site at a time, and using the left block from the previous left-to-right sweep.
- Re-iterate the sweeping. Stop when the change in the energy is below a predefined tolerance. One typically stops at a point when both blocks have the same size, the "symmetric configuration".

This sweeping process works in a similar fashion as a self-consistent loop, where we iteratively improve the solution. In fact, the DMRG can be formulated as a variational method, in which the variational parameters are continuously improved to minimize an energy functional. Intuitively a way to see it is by imagining a "demon" probing the environment around the block for the optimal states to improve the basis to represent the ground-state. These states are "absorbed" inside the block by the density matrix and its eigenvectors.

As described above, the shrinking block is replaced by the block from the previous sweep in the opposite direction. This means that all the information about the block and its operators needs to be stored, either in memory, or dumped on disk.

2.5.1 Obtaining Quasi-Exact Results with the Finite-Size DMRG

The DMRG accuracy is parametrized by a quantity called the "truncation error", which is nothing but the residue of the trace of the density matrix after the truncation, Eq. (2.32). This is equal to the sum of the eigenvalues of the discarded states. How well the DMRG performs for a particular problem, and how many states we need to keep in order to achieve the desired accuracy will depend on the behavior of the eigenvalues of the density matrix, something that we will discuss in another section below. We say that the DMRG results are quasi-exact when the accuracy is strictly controlled by the truncation error, and can be improved by increasing the number of states kept m. However, even though the DMRG guarantees that we can obtain quasi-exact results, there are many other factors that need to be taken into account to make sure that the simulation has properly converged. Failing to do so may produce biased results. In order to avoid "mistakes" when using the DMRG, we should pay attention to the following:

- Applying the infinite-size DMRG to finite systems is not quasi-exact, and this has been the source of many mistakes in the past. Sweeping is an essential step in order to get accurate results, and multiple sweeps are typically required. A way to make sure that convergence is achieved is by looking at observables as we sweep, and making sure that they respect the symmetries of the problem. For instance, in a uniform spin chain, correlations from the end sites or the central sites should be

symmetric under reflections. Typically, observables do not converge as fast as the energy. Errors in the correlations tend to be higher than errors in the energy.

- A typical analysis of the results consists of looking at the behavior of the energy and observables as a function of the number of states kept m. Sometimes, in challenging situations that requires large numbers of states to converge, an extrapolation with m or the truncation error can be attempted.
- In cases where our computer power allows, we can typically guarantee well converged results by fixing the truncation error beforehand. We can ask the algorithm to automatically increase the number of states m such that the truncation error always lies within a tolerance.
- A finite-size scaling requires well converged results for every system size. Poor results for large system sizes can seriously bias the extrapolations and analysis.
- In some peculiar cases it may happen that the system gets trapped in a local minimum. This may occur for several reasons. A common one is doing the warmup or infinite-size sweep with too few states. This problem usually arises in calculations in momentum space, or with large barriers between energy manifolds, or in proximity to a first order first transition. A way to avoid this "sticking" problem is by adding a source of randomness in the density matrix that may induce the fluctuations necessary to escape the meta-stable state. Another possibility is by introducing fluctuations in some parameter of the model.
- Ultimately, the energy and ground-state are obtained by means of the Lanczos or Davidson diagonalization. It is essential that the diagonalization step is performed with an accuracy superior to the truncation error. Otherwise, the diagonalization errors will dominate over the truncation error, and the ground state will not have the expected accuracy, and may actually include a mixture of excited states (In fact, this may always happen to a certain extent, but a poor diagonalization may magnify the effects of the truncation).

2.5.2 Measuring Observables

Let us assume that we have a one-dimensional chain of certain length, and we want to measure correlations between observables acting on different sites, O_i and O'_j. Two cases can arise: (i) both sites are in separate blocks, or (ii) the two sites are inside the same block. Whether we find ourselves in situation (i) or (ii) will depend on the stage of the sweep. Sometimes we may find that the situation (i) will happen, and sometimes (ii). As we are going to see next, it is more convenient to measure the observables in case (i).

Operators in Separate Blocks

Let us assume a generic situation during the sweep where we find the two operators on separate blocks, as illustrated in Fig. 2.11. Let us denote the basis states for the

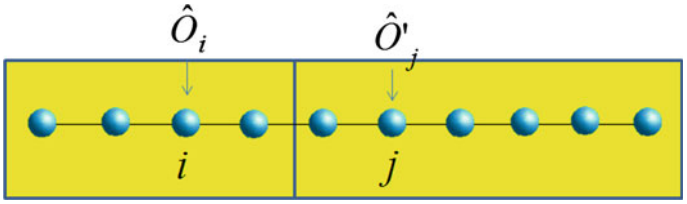

Fig. 2.11 Setup for measuring observables acting on sites in separate blocks

left block as $\{|\alpha\rangle\}$, and for the right block as $\{|\beta\rangle\}$. The ground state wave-function will be give as:

$$|\Psi\rangle = \sum_{\alpha\beta} \langle\alpha\beta|\Psi\rangle|\alpha\beta\rangle = \sum_{\alpha\beta} \Psi_{\alpha\beta}|\alpha\beta\rangle. \tag{2.46}$$

It is easy to see that the correlation can be obtained as:

$$\begin{aligned}\langle \hat{O}_i \hat{O}'_j\rangle &= \langle\Psi|\hat{O}_i \hat{O}'_j|\Psi\rangle \\ &= \sum_{\alpha\beta,\alpha'\beta'} \Psi^*_{\alpha'\beta'}\Psi_{\alpha\beta}\langle\alpha'\beta'|\hat{O}_i \hat{O}'_j|\alpha\beta\rangle \\ &= \sum_{\alpha\beta,\alpha'\beta'} \Psi^*_{\alpha'\beta'}\Psi_{\alpha\beta}\langle\alpha'|\hat{O}_i|\alpha\rangle\langle\beta'|\hat{O}'_j|\beta\rangle \\ &= \sum_{\alpha\beta,\alpha'\beta'} \Psi^*_{\alpha'\beta'}\Psi_{\alpha\beta}(\tilde{O}_i)_{\alpha\alpha'}(\tilde{O}'_j)_{\beta\beta'}.\end{aligned} \tag{2.47}$$

Operators in the Same Block

The situation with both operators in the same block is illustrated in Fig. 2.12. The proper way to calculate the correlations it by defining the composite product operator $\hat{O}_{ij} = \hat{O}_i \hat{O}'_j$. The correlation is then expressed as:

$$\begin{aligned}\langle \hat{O}_i \hat{O}'_j\rangle &= \langle\Psi|\hat{O}_i \hat{O}'_j|\Psi\rangle = \langle\Psi|\hat{O}_{ij}|\Psi\rangle \\ &= \sum_{\alpha\beta,\alpha'\beta'} \Psi^*_{\alpha'\beta'}\Psi_{\alpha\beta}\langle\alpha'|\hat{O}_{ij}|\alpha\rangle\langle\beta'|\beta\rangle \\ &= \sum_{\alpha\beta,\alpha'} \Psi^*_{\alpha'\beta}\Psi_{\alpha\beta}(\tilde{O}_{ij})_{\alpha\alpha'}.\end{aligned} \tag{2.48}$$

We clearly see that the composite operator has to be stored in the block, together with the individual operators. We need to represent it in the rotated basis the same as we do for the Hamiltonian when we do the truncation. Calculating this quantity

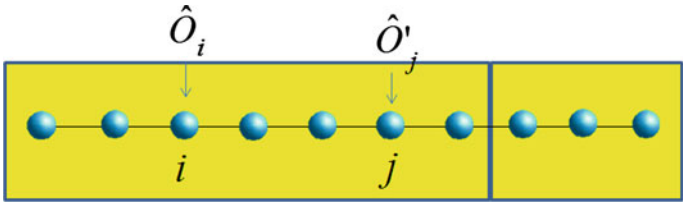

Fig. 2.12 Setup for measuring observables acting on sites in the same block

as the product of two individual operators in the truncated basis is bad practice and should be avoided.

Clearly, storing and propagating the product operators for all pairs acting on sites i and j can be computationally very expensive. It is therefore convenient to store the individual operators, and calculate the correlations only when the operators are in separate blocks, as illustrated before.

2.5.3 Targeting States

It is important to point out that our basis has been optimized to accurately represent only the ground state. If we wanted to calculate other states, such as excited states, we need to build the density matrix using all these states as "target" states:

$$\rho = \sum_t w_t |\Psi_t\rangle\langle\Psi_t| \tag{2.49}$$

which is equivalent to the density matrix of a mixed state, with weights w_t, such that $\sum_t w_t = 1$. Finding a good combination of weights is a matter of trial and error, and it may depend on the particular problem. Generally, one picks all the weights to be equal.

When one targets multiple states, the number of DMRG states that we need to keep in order to represent them with enough accuracy grows in the same proportion.

2.5.4 Calculating Excited States

Sometimes we are interested in calculating excited states in sectors with different symmetry than the ground state. For instance, we may want to obtain the singlet-triplet gap by calculating the ground states in sectors with well defined total spin $S = 0$ and $S = 1$. If we could use the symmetries of the Hamiltonian to be able to restrict our calculation to a sector with well-defined quantum numbers, then this should not be a problem. In these notes we are leaving the discussion on the use of

symmetries aside for the moment. So the problem now is to obtain the excited states, regardless of their quantum numbers. In this case we apply a simple trick that is also used in exact diagonalization calculations: At every step during the simulation, we target the ground state $|\Psi\rangle$ of the Hamiltonian of interest $\hat{H}$, and the ground state $|\Psi_1\rangle$ of the modified Hamiltonian:

$$\hat{H}' = \hat{H} + \Lambda|\Psi\rangle\langle\Psi|. \tag{2.50}$$

We have introduced a projector on the ground state that shifts its energy by an amount proportional to a constant Λ, that we pick to be sufficiently large. As a result, the ground state will be shifted in energy to the top of the spectrum, leaving the first excited state as the new ground state. As we explained before, in order to accurately represent both states, we need to use the density matrix:

$$\rho = \frac{1}{2}|\Psi\rangle\langle\Psi| + \frac{1}{2}|\Psi_1\rangle\langle\Psi_1|. \tag{2.51}$$

2.5.5 Wave-Function Prediction

At every step of the sweep we find that we have to obtain the ground-state of the Hamiltonian using some suitable diagonalization routine (Lanczos, Davidson). These algorithms converge iteratively to the ground-state, typically starting from some random seed. Depending on the accuracy wanted, one would have to perform a number of iterations, say between 20 and 100, applying the Hamiltonian to a new state at every iteration, until convergence is achieved. White [24] realized that the process could be sped up if we use the ground state from the previous step in the sweeping, as a starting seed for the diagonalization. All one would have to do is transform the old ground-state to the new basis. This process is usually referred to as "wave-function prediction" or "wave-function transformation".

We assume we obtained the ground-state of our Hamiltonian, which before the change of basis is written as (see Fig. 2.13):

$$|\Psi\rangle = \sum_{\alpha_i, s_{i+1}, s_{i+2}, \beta_{i+3}} \langle \alpha_i s_{i+1} s_{i+2} \beta_{i+3} | \Psi \rangle | \alpha_i s_{i+1} s_{i+2} \beta_{i+3} \rangle \tag{2.52}$$

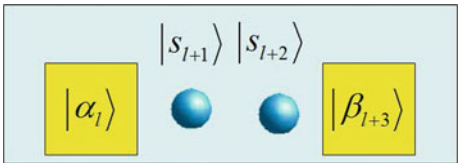

Fig. 2.13 Four blocks used to represent the ground-state wave-function for the wave-function transformation

After the change of basis, we add a site to the left block, and we "spit out" one from the right block:

$$|\Psi\rangle = \sum_{\alpha_{i+1},s_{i+2},s_{i+3},\beta_{i+4}} \langle \alpha_{i+1} s_{i+2} s_{i+3} \beta_{i+4} | \Psi \rangle | \alpha_{i+1} s_{i+2} s_{i+3} \beta_{i+4} \rangle \tag{2.53}$$

After some algebra, and assuming that $\sum_{\alpha_i} |\alpha_i\rangle\langle\alpha_i| \approx 1$ and $\sum_{\beta_i} |\beta_i\rangle\langle\beta_i| \approx 1$ after the truncation, one can readily obtain:

$$\begin{aligned} \langle \alpha_{i+1} s_{i+2} s_{i+3} \beta_{i+4} | \Psi \rangle &\approx \sum_{\alpha_i, s_{i+1} \beta_{i+3}} \langle \alpha_{i+1} | \alpha_i s_{i+1} \rangle \langle s_{i+3} \beta_{i+4} | \beta_{i+3} \rangle \langle \alpha_i s_{i+1} s_{i+2} \beta_{i+3} | \Psi \rangle \\ &= \sum_{\alpha_i, s_{i+1} \beta_{i+3}} (U_L^\dagger)_{\alpha_{i+1}, \alpha_i s_{i+1}} (U_R)_{s_{i+3} \beta_{i+4}, \beta_{i+3}} \langle \alpha_i s_{i+1} s_{i+2} \beta_{i+3} | \Psi \rangle \end{aligned} \tag{2.54}$$

This operation has relatively little computational cost, especially after considering that it will reduce the ground-state calculation to just a few Lanczos or Davidson iterations.

2.5.6 Generalization to Higher Dimensions and Complex Geometries

The DMRG method was originally introduced to study one dimensional systems. However, it can be extended to higher dimensions in a very straightforward way [25, 26]. Consider for simplicity a system of orbitals in a rectangular arrangement, as shown in Fig. 2.14, with first neighbor interactions, only. We can draw an imaginary path that scans through the lattice following a "snake"-like pattern. We can stretch the snake by putting all the orbitals aligned in a one-dimensional arrangement, and we obtain a system that we can study with the conventional DMRG. There is, however, a price tag to this simplification: the interactions now have long-range.

Other possible solutions have been explored in the literature. For instance, one could choose a vertical band composed by several sites along the y direction, and use the one-dimensional scheme in this super-site basis [27]. Another possibility is to use a different snake-like path that still adds one site at a time, but scans through the lattice more symmetrically [28]. Whatever the preferred solution is, in two-dimensional systems we always find the same barrier: entanglement grows with the size of the boundaries between left and right blocks. This affects the behavior of the density matrix spectrum, and as it turns out, we need to keep more DMRG states to achieve good results. The justification for this behavior will be explained in the following sections. For now, we simply point out that using "cylindrical" boundary conditions, with open boundary conditions along the x direction, and periodic along y, is the preferred setup for two-dimensional problems.

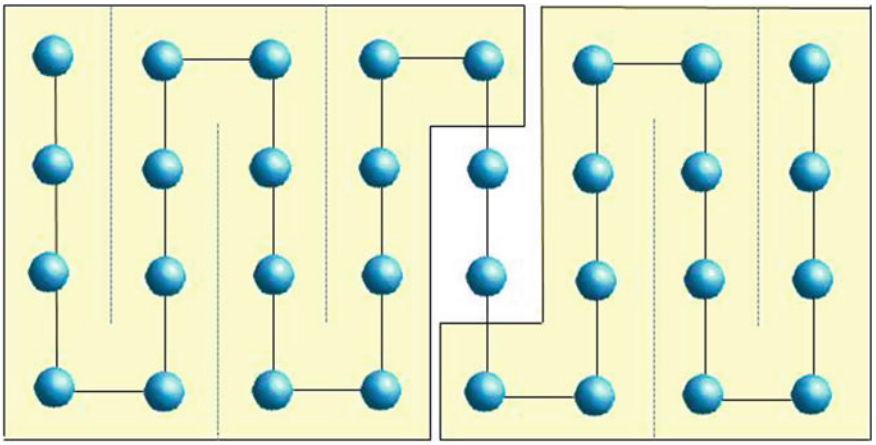

Fig. 2.14 Generalizing the DMRG to 2d implies defining a one-dimensional path through the lattice

2.6 When and Why Does the DMRG Work?

While experimenting with the newly discovered method, Steve White noticed systems with periodic boundary conditions were ill-behaved: in order to achieve a given accuracy for a simple one-dimensional model with periodic boundary conditions would require, for instance $O(10^4)$ states, while for the case of open boundary conditions, one could get away with just a fraction of those, say $O(10^2)$. He experimented with several approaches, but in the end, in seemed as though the only way to deal with this situation was by brute force, keeping lots of states. The reason for these different behaviors was somewhat a mystery, and it remained so until recently, when the quantum information community started exploring algorithms for simulating quantum many body problems (similar to the DMRG) [29, 30], and this behavior was finally understood. These ideas rely on the concept of "quantum entanglement" [31–33], and understanding how much information is needed to represent a quantum state faithfully can be quantified in terms of an "entanglement entropy" [34]. Quantum information could now explain why certain systems behaved in a certain way, depending on the geometry and topology of the lattice, by understanding the behavior of the spectrum of the reduced density matrices.

2.6.1 Entanglement

Entanglement is a property of quantum mechanical states composed of two or more "objects": since in quantum mechanics the state of a system can be described as a linear superposition of basis states, we find that most of the time, we cannot describe

the state of an object, or a part of the system, without knowledge of the rest. To illustrate this idea let us consider the simple case of two spins, and assume there state can be described as:

$$|\Psi\rangle = |\uparrow\uparrow\rangle + |\uparrow\downarrow\rangle + |\downarrow\uparrow\rangle + |\downarrow\downarrow\rangle \tag{2.55}$$

We can readily see that this is equivalent to

$$\Psi\rangle = (|\uparrow\rangle + |\downarrow\rangle) \otimes (|\uparrow\rangle + |\downarrow\rangle) \tag{2.56}$$

Therefore, even though we started from a state that seemed to have a complicated structure, we found that in reality the two spins are not entangled: their wave-function can be written as the product of the states of the two individual spins. The two spins carry information individually, and knowing the state of one spin, does not tell us anything about the state of the second spin.

Instead, the following wave-function

$$|\Psi\rangle = |\uparrow\downarrow\rangle + |\downarrow\uparrow\rangle \tag{2.57}$$

cannot be separated: if we look at one spin, and it is pointing in one direction, we know that the other spin will be pointing in the opposite direction. In fact, for this particular example, the state of one spin carries *all* the information about the state of the second spin. We are going to see later that this case is referred to as the "maximally entangled" state of the two spins.

2.6.2 Entanglement and the Schmidt Decomposition

Let us assume that we define a partition in our system into parts A and B, same as we have been doing it all along during our discussion. The generic state of our system can be expressed, once more, as:

$$|\Psi\rangle = \sum_{ij} \Psi_{ij} |i\rangle |j\rangle, \tag{2.58}$$

where the states $\{|i\rangle\}$ and $\{|j\rangle\}$ live on parts A and B, and have dimensions D_A and D_B, respectively. This means that in order to describe the problem we need to know $D_A \times D_B$ complex coefficients.

Let us re-formulate the original DMRG premise: Can we simplify this state by changing to a new basis? And… what do we mean by "simplifying" the state, anyway?

We have seen, that through a SVD decomposition, we can re-write the state as:

$$|\Psi\rangle = \sum_{\alpha}^{r} \lambda_\alpha |\alpha\rangle |\alpha\rangle \tag{2.59}$$

where $r = \min(D_A, D_B)$, $\lambda_\alpha \geq 0$, and the states $\{|\alpha\rangle_A\}$ and $\{|\alpha\rangle_B\}$ form an orthogonal basis for the subsystems.

We notice right away, that if the Schmidt rank $r = 1$, then the wave-function reduces to a product state, "disentangling" the two subsystems.

How accurately or faithfully we will be able to represent the state by truncating the basis, will clearly depend on the behavior of the Schmidt coefficients λ_α. If we recall that these are related to the eigenvalues of the reduced density matrices as $\omega_\alpha = \lambda_\alpha^2$, we conclude that the efficiency of the DMRG will be completely determined by the spectrum of the reduced density matrices, the so-called "entanglement spectrum":

- If the eigenvalues decay very fast (exponentially, for instance), then we introduce little error by discarding the smaller ones.
- Few coefficients mean less entanglement. In the extreme case of a single non-zero coefficient, the wave-function is a product state and completely disentangled.
- The same way NRG minimizes the energy… DMRG minimizes the loss of information! The closer the state resembles a product state, the more efficient our truncation will be. Let us be clear, the amount of entanglement is in reality always the same, but when we rotate to a new basis, we pick it in such a way that the Schmidt coefficients are concentrated in as few states as possible, so we can discard the rest with a minimum loss of information.

2.6.3 Quantifying Entanglement

In order to quantify the entanglement, we define a quantity called the "entanglement entropy". There are many definition, we shall pick the so called "von Neumann entanglement entropy":

$$S = -\sum_{\alpha} \lambda_\alpha^2 \log \lambda_\alpha^2. \tag{2.60}$$

Or, in terms of the reduced density matrix:

$$S = -\mathrm{Tr}\left(\rho_A \log \rho_A\right) = -\mathrm{Tr}\left(\rho_B \log \rho_B\right). \tag{2.61}$$

To illustrate what this quantity represents, let us look again at the normalized state:

$$|\Psi\rangle = \frac{1}{\sqrt{2}}\left[|\uparrow\downarrow\rangle + |\downarrow\uparrow\rangle\right]. \tag{2.62}$$

We can obtain the reduced density matrix for the first spin, by tracing over the second spin

$$\rho = \begin{pmatrix} 1/2 & 0 \\ 0 & 1/2 \end{pmatrix} \tag{2.63}$$

We say that the state is "maximally entangled" when the reduced density matrix is proportional to the identity. The entanglement entropy in this case is:

$$S = -\frac{1}{2}\log\frac{1}{2} - \frac{1}{2}\log\frac{1}{2} = \log 2. \tag{2.64}$$

In general, if the rank of the Schmidt decomposition is $r = \min(D_A, D_B)$, then the entanglement spectrum will be $\omega_\alpha = 1/r$, and the entanglement entropy of the maximally entangled state will be $S = \log r$.

If the state is a product state:

$$|\Psi\rangle = |\alpha\rangle|\beta\rangle. \tag{2.65}$$

All the eigenvalues of the reduced density matrices will be $\omega_\alpha = 0$ except for one $\omega_1 = 1$, and the entanglement entropy will be $S = 0$.

2.6.4 The Area Law

We know understand how to quantify the accuracy of the DMRG in terms of entanglement. What we still do not understand is why the DMRG performs so well in one-dimensional cases, and not so-well in two dimensions, and in systems with periodic boundary conditions. We can see that these issues have to be somehow related to the behavior of the entanglement spectrum, and there must be something that makes it behave in a particular way for some problems.

The study of the entanglement properties of quantum systems is a relatively new subject. It has recently become very relevant in condensed matter due to its ability to characterize quantum many body systems. As it turns out, it can be shown that the ground states of certain Hamiltonians, under certain conditions, obey what is called "area laws" for the entanglement entropy [35]. That is why the entanglement entropy is sometimes also called "geometric entropy". This is now a topic of intense research and in these nodes we shall only described the main ideas in a qualitative way.

Consider the ground-state of a local Hamiltonian (with interactions limited to close neighbors). In two spacial dimensions, that is pictorially shown in Fig. 2.15. This state represents what is commonly known as a valence bond solid, in which some bonds form strong singlets (2.57). These singlets are represented in the figure by thick lines. Let us now draw an imaginary partition, as shown with the gray shaded area. The boundary lines will cut a number of singlets, proportional to the length, or perimeter of the partition. Since we know that the entanglement entropy between two spins forming a singlet is log(2), we conclude that the entanglement entropy between the enclosed region and the outside will be

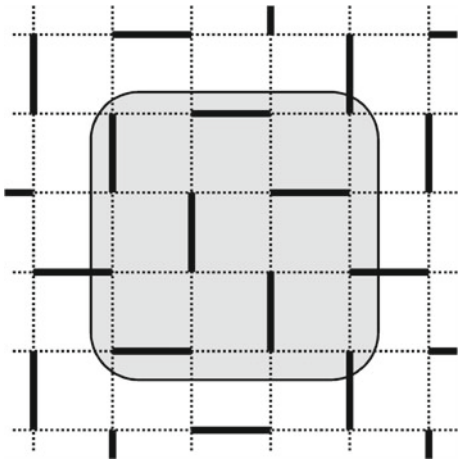

Fig. 2.15 Schematic representation of a valence bond solid. *Thick lines* represent singlets

$$S = \log(2) \times (\#\text{ of bonds cut}) \approx L \log(2) \tag{2.66}$$

Hence, the entanglement entropy is proportional to the area of the boundary separating both regions. This is the prototypical behavior of gaped systems, which we illustrate with this simple example [36]. The same ideas can be generalized to other contexts. Notice that this means that in *gaped* one-dimensional systems, the entanglement entropy between two pieces, left and right, is independent of the size of the partition (again, we are referring to models with short range interactions).

It can be shown using conformal field theory arguments [37, 38], that the entanglement entropy of *critical* (gapless) one-dimensional system with periodic boundary conditions obeys the law:

$$S \sim \frac{c}{3} \log(L) \tag{2.67}$$

where c is the "central charge" of the system, a measure of the number of gapless modes. For the case of open boundary conditions, a similar expression is obtained:

$$S \sim \frac{c}{6} \log(L) \tag{2.68}$$

The factor 2 arises from the simple fact that a system with periodic boundary conditions has *two* boundaries, compared to one in the case of open boundary conditions.

In general, most systems obey the area law, with some exceptions such as free fermions, or fermionic systems with a 1D Fermi surface [39–42].

2.6.5 Entanglement and the DMRG

In general, the number of DMRG state that we need to keep to represent a state is related to the entanglement entropy between the two blocks as [34, 43]:

$$m \approx \exp(S) \tag{2.69}$$

Therefore, we can predict the behavior or the algorithm for certain classes of systems:

- Gaped systems in 1D: $m = const.$
- Critical systems in 1D: $m \approx L^{\alpha}$.
- Gaped systems in 2D: $m = \exp(L)$.
- Periodic boundary conditions in 1D: we need to keep the square of the states needed for open boundary conditions, since the boundary area is now doubled.

These rules of thumb give an idea of the computational cost of a simulation. However, the entanglement entropy is not the only factor that determines the behavior of the DMRG, but also the internal structure of the wave function which has the form of a matrix product state [10–13, 44]. This will be discussed in detail in a separate chapter of the book.

2.7 Outlook: DMRG and Tensor Network Methods

With the advent of matrix product state algorithms, and quantum information ideas, we have seen a remarkable progress in the computational field. A repeated question that arises is whether the variational approaches using MPS are more efficient, or "better" that conventional DMRG. The short answer is "not necessarily". If one is interested in studying one-dimensional problems, all methods are basically equivalent. One may argue that MPS algorithms work better for periodic boundary conditions [45, 46], but the drawback is that the implementation of the MPS code suffers from normalization problems that may lead to some instabilities. It is possible to reformulate the DMRG as an MPS optimization code [47], that may lead to a hybrid solution. What is certain is that most of the people that have been working with the DMRG for decades, have very polished, optimized, state-of-the-art codes that are hard to beat with existent MPS codes. However, progress is rapidly being made, and ultimately, it may become a matter of taste. DMRG may be easier to generalize to arbitrary Hamiltonians, and general purpose codes exist and are freely available, such as the ALPS DMRG code [48–50]. On the other hand, MPS's enjoy several advantages that in the end may make them the favorite choice: They are probably easier to understand intuitively; one only has to store local matrices; the structure of the wavefunction is easy to deal with algebraically; they are easy to extend to the thermodynamic limit in translational invariant problems [51–54]; overlaps between MPS's are easy to calculate; and most importantly, the MPS structure makes them more suitable for massive parallellization, especially for time-evolution [55–57].

MPS's are extremely powerful objects, and we have been learning a great deal about entanglement [43], complexity [58–60], and the structure of the quantum world through them [61]. The concept can readily be extended to higher dimensions, with matrices being replaced by tensors, leading to complex structures: tensor networks. Several ideas exploiting tensor networks have been proposed, such as PEPS (projected entangled pair states) [54] and MERA (multi-scale entanglement renormalization ansatz) [62–65], with very promising results. However, until recent work [66], DMRG has always been more efficient at studying 2D problems [67]. The main reason for this is, once more, the lack of highly optimized code to deal with the tensor contractions in PEPS, which is a complex computational problem [68–70], and in the case of MERA, with the explicit breaking of the translational symmetry. But again, progress is rapidly being made, and we can anticipate a new wave of computational methods based on tensor network methods.

References

1. F.D.M. Haldane, Phys. Lett. **80A**, 281 (1980)
2. T.C. Choy, Phys. Lett. **80A**, 49 (1980)
3. See also S.R. Manmana et al., Phys. Rev. A **84**, 043601 (2011)
4. R.B. Laughlin, Phys. Rev. Lett. **50**, 1395 (1983)
5. R. Schrieffer, *Theory of Superconductivity*, Advanced Books Classics (Perseus, Chicago, 1999)
6. S.R. White, Phys. Rev. Lett. **69**, 2863 (1992)
7. S.R. White, Phys. Rev. B **48**, 10345 (1993)
8. K.G. Wilson, Rev. Mod. Phys. **47**, 773 (1975)
9. R. Bulla, T.A. Costi, T. Pruschke, Rev. Mod. Phys. **80**, 395 (2008)
10. S. Ostlund, S. Rommer, Phys. Rev. Lett. **75**, 3537 (1995)
11. S. Rommer, S. Ostlund, Phys. Rev. B **55**, 2164 (1997)
12. H.A. Kramers, G.H. Wannier, Phys. Rev. **60**, 263 (1941)
13. R.J. Baxter, J. Math. Phys. **9**, 650 (1968)
14. I. Peschel, X. Wang, M. Kaulke, K. Hallberg (eds.), *Density-Matrix Renormalization—A New Numerical Method in Physics: Lectures of a Seminar and Workshop held at the Max-Planck-Institut für Physik*, Lecture Notes in Physics (Springer, Berlin, 1999)
15. U. Schollwöck, Rev. Mod. Phys. **77**, 259 (2005)
16. K. Hallberg, Density matrix renormalization: a review of the method and its applications, in *Theoretical Methods for Strongly Correlated Electrons*, CRM Series in Mathematical Physics, ed. by D. Senechal, A.-M. Tremblay, C. Bourbonnais (Springer, New York, 2003)
17. K. Hallberg, Adv. Phys. **55**, 477 (2006)
18. R.M. Noack, S.R. Manmana, Proceedings of the "IX. Training course in the physics of correlated electron systems and high-Tc superconductors", Vietri sul Mare (Salerno, Italy, October 2004). AIP Conf. Proc. **789**, 93 (2005)
19. G. De Chiara, M. Rizzi, D. Rossini, S. Montangero, J. Comput. Theor. Nanosci. **5**, 1277 (2008)
20. A.E. Feiguin, Proceedings of the "XV. Training course in the physics of correlated electron systems", Vietri sul Mare (Salerno, Italy, October 2010). AIP Conf. Proc. **1419**, 5 (2011)
21. A.C. Hewson, *The Kondo Problem to Heavy Fermions* (Cambridge University Press, Cambridge, 1997)
22. C. Lanczos, J. Res. Natl. Bur. Stand. **45**, 255 (1950)
23. D.G. Pettifor, D.L. Weaire (eds.), *The Recursion Method and Its Applications*, Springer Series in Solid State Sciences, vol. 58 (Springer, Berlin, 1985)

24. S.R. White, Phys. Rev. Lett. **77**, 3633 (1996)
25. R.M. Noack, S.R. White, D.J. Scalapino, The density-matrix renormalization group for fermion systems, in *Computer Simulations in Condensed Matter Physics*, vol. VII, ed. by D.P. Landau, K.K. Mon, H.B. Schüttler (Spinger, Heidelberg, 1994), UCI-CMTHE-94-03
26. S. Liang, H. Pang, Europhys. Lett. **32**, 173 (1995)
27. M.S.L. du Croo de Jongh, J.M.J. van Leeuwen, Phys. Rev. B **57**, 8494 (1998)
28. T. Xiang, J.Z. Lou, Z.B. Zu, Phys. Rev. B **64**, 104414 (2001)
29. G. Vidal, Phys. Rev. Lett. **91**, 147902 (2003)
30. G. Vidal, Phys. Rev. Lett. **93**, 040502 (2004)
31. M.B. Plenio, S. Virmani, Quantum Inf. Comput. **7**, 1 (2007)
32. L. Amico, R. Fazio, A. Osterloh, V. Vedral, Rev. Mod. Phys. **80**, 517 (2008)
33. R. Horodecki, P. Horodecki, M. Horodecki, K. Horodecki, Rev. Med. Phys. **81**, 865 (2009)
34. F. Verstraete, J.I. Cirac, Phys. Rev. B **73**, 094423 (2006)
35. J. Eisert, M. Cramer, M.B. Plenio, Rev. Mod. Phys. **82**, 277 (2010)
36. M.B. Hastings, J. Stat. Mech.: Theory Exp. **2007**, P08024 (2007)
37. P. Calabrese, J. Cardy, J. Stat. Mech.: Theory Exp. **2004**, P06002 (2004)
38. P. Calabrese, J. Cardy, Int. J. Quantum Inf. **4**, 429 (2006)
39. M.M. Wolf, Phys. Rev. Lett. **96**, 010404 (2006)
40. D. Gioev, I. Klich, Phys. Rev Lett. **96**, 100503 (2006)
41. W. Li, L. Ding, R. Yu, T. Roscilde, S. Haas, Phys. Rev. B **74**, 073103 (2006)
42. T. Barthel, M.-C. Chung, U. Schollwöck, Phys. Rev. A **74**, 022329 (2006)
43. F. Verstraete, M.M. Wolf, D. Perez-Garcia, J.I. Cirac, Phys. Rev. Lett. **96**, 220601 (2006)
44. U. Schollwöck, Ann. Phys. **326**, 96 (2011)
45. F. Verstraete, D. Porras, J.I. Cirac, Phys. Rev. Lett. **93**, 227205 (2004)
46. See also P. Pippan, S.R. White, H.G. Evertz, Phys. Rev. B **81**, 081103 (2010)
47. I. McCulloch, J. Stat. Mech. **2007**, P10014 (2007)
48. B. Bauer et al. (ALPS collaboration), J. Stat. Mech. **2011**, P05001 (2011)
49. F. Albuquerque et al. (ALPS collaboration), J. Magnet. Magnet. Mater. **310**, 1187 (2007)
50. F. Alet et al. (ALPS collaboration), J. Phys. Soc. Jpn. Suppl. **74**, 30 (2005)
51. R. Orus, G. Vidal, Phys. Rev. B **78**, 155117 (2008)
52. I.P. McCulloch, arXiv:0804.2509
53. B. Pirvu, F. Verstraete, G. Vidal, Phys. Rev. B **83**, 125104 (2011)
54. J. Jordan, R. Orus, G. Vidal, F. Verstraete, J.I. Cirac, Phys. Rev. Lett. **101**, 250602 (2008)
55. M.C. Bañuls, M.B. Hastings, F. Verstraete, J.I. Cirac, Phys. Rev. Lett. **102**, 240603 (2009)
56. I. Pizorn, L. Wang, F. Verstraete, Phys. Rev. A **83**, 052321 (2011)
57. M.B. Hastings, J. Math. Phys. **50**, 095207 (2009)
58. N. Schuch, M.M. Wolf, F. Verstraete, J.I. Cirac, Phys. Rev. Lett. **100**, 030504 (2008)
59. N. Schuch, M.M. Wolf, F. Verstraete, J. Ignacio Cirac, Phys. Rev. Lett. **98**, 140506 (2007)
60. N. Schuch, I. Cirac, F. Verstraete, Phys. Rev. Lett. **100**, 250501 (2008)
61. F. Verstraete, J.I. Cirac, Phys. Rev. Lett. **104**, 190405 (2010)
62. G. Vidal, Phys. Rev. Lett. **99**, 220405 (2007)
63. G. Evenbly, G. Vidal, Phys. Rev. B **79**, 144108 (2009)
64. G. Evenbly, G. Vidal, Phys. Rev. Lett. **102**, 180406 (2009)
65. G. Vidal, in *Understanding Quantum Phase Transitions*, ed. by L.D. Carr (Taylor & Francis, Boca Raton, 2010)
66. P. Corboz, S.R. White, G. Vidal, M. Troyer, arXiv:1104.5463
67. S. Yan, D.A. Huse, S.R. White, Science **332**, 1173 (2011)
68. Gu Zheng-Cheng, Michael Levin, Xiao-Gang Wen, Phys. Rev. B **78**, 205116 (2008)
69. Z.Y. Xie, H.C. Jiang, Q.N. Chen, Z.Y. Weng, T. Xiang, Phys. Rev. Lett. **103**, 160601 (2009)
70. H.H. Zhao, Z.Y. Xie, Q.N. Chen, Z.C. Wei, J.W. Cai, T. Xiang, Phys. Rev. B **81**, 174411 (2010)

http://www.springer.com/978-3-642-35105-1

Strongly Correlated Systems
Numerical Methods
Avella, A.; Mancini, F. (Eds.)
2013, XXVIII, 325 p., Hardcover
ISBN: 978-3-642-35105-1